ADVANCED MATERIALS
www.advmat.de

Antimicrobial Microwebs of DNA–Histone Inspired from Neutrophil Extracellular Traps

Yang Song, Usha Kadiyala, Priyan Weerappuli, Jordan J. Valdez, Srilakshmi Yalavarthi, Cameron Louttit, Jason S. Knight, James J. Moon, David S. Weiss, J. Scott VanEpps, and Shuichi Takayama**

Neutrophil extracellular traps (NETs) are decondensed chromatin networks released by neutrophils that can trap and kill pathogens but can also paradoxically promote biofilms. The mechanism of NET functions remains ambiguous, at least in part, due to their complex and variable compositions. To unravel the antimicrobial performance of NETs, a minimalistic NET-like synthetic structure, termed "microwebs," is produced by the sonochemical complexation of DNA and histone. The prepared microwebs have structural similarity to NETs at the nanometer to micrometer dimensions but with well-defined molecular compositions. Microwebs prepared with different DNA to histone ratios show that microwebs trap pathogenic *Escherichia coli* in a manner similar to NETs when the zeta potential of the microwebs is positive. The DNA nanofiber networks and the bactericidal histone constituting the microwebs inhibit the growth of *E. coli*. Moreover, microwebs work synergistically with colistin sulfate, a common and a last-resort antibiotic, by targeting the cell envelope of pathogenic bacteria. The synthesis of microwebs enables mechanistic studies not possible with NETs, and it opens new possibilities for constructing biomimetic bacterial microenvironments to better understand and predict physiological pathogen responses.

Nature uses a variety of extracellular nanofibers, such as cobwebs,[1] amyloid plaques,[2] and fibrin clots[3] to capture invading microbes. As part of human innate immunity, neutrophils squirt decondensed chromatin networks to capture and disarm bacteria and fungi—a host defense process known as "NETosis"[4] (**Figure 1**a). Such endogenous networks, named neutrophil extracellular traps (NETs; Figure 1b), are composed of meshes of DNA strands and histone, decorated with antimicrobial protein granules and enzymes.[5] NETs have been observed to be lethal to a number of bacteria,[6] fungi,[7] viruses,[8] and parasites,[9] yet some pathogenic bacteria can evade NET-induced killing.[10,11] Accumulation of excessive NETs in vivo is also associated with pathology of bacterial biofilm, autoimmune disease, and even cancer.[12] These complex and sometimes contradictory observations highlight the need to investigate NET-related physiological interactions with simpler but defined NET-like biomaterials.

Isolation of NETs from neutrophils requires repeated centrifugation and washing steps,[13] which often causes unpredictable loss of proteins. Moreover, NETs can be triggered via chemical stimulus,[14] virulence factors,[15] and bacteria[16] under different pathways, yielding 33 common proteins and as much as 50 variable proteins.[12] While the existing antibodies and inhibitors are employed to block and characterize the function of specific NET components, their high complexity imposes limitations.[17] Here, we take a bottom-up approach of synthesizing NET-like materials with defined composition, termed "microwebs," through sonochemical complexation of lambda phage DNA and histone in aqueous solutions. Lambda phage DNA can spontaneously polymerize into networks in the presence of histone,[18] which facilitates formation of web-like structure. *Escherichia coli UTI89* was used as a model pathogen

Dr. Y. Song, Prof. S. Takayama
Wallace H Coulter Department of Biomedical Engineering & Petit Institute for Bioengineering and Bioscience
Georgia Institute of Technology & Emory School of Medicine
Atlanta, GA 30332, USA
E-mail: takayama@gatech.edu

U. Kadiyala, Dr. J. S. VanEpps
Department of Emergency Medicine
Michigan Center for Integrative Research in Critical Care
Biointerfaces Institute
University of Michigan
Ann Arbor, MI 48109, USA
E-mail: jvane@med.umich.edu

The ORCID identification number(s) for the author(s) of this article can be found under https://doi.org/10.1002/adma.201807436.

DOI: 10.1002/adma.201807436

P. Weerappuli, C. Louttit, Dr. J. J. Moon
Department of Biomedical Engineering
University of Michigan
Ann Arbor, MI 48109, USA

J. J. Valdez, Dr. D. S. Weiss
Emory Antibiotic Resistance Center
Emory Vaccine Center
School of Medicine
Emory University
Atlanta, GA 30307, USA

Dr. S. Yalavarthi, Dr. J. S. Knight
Division of Rheumatology
University of Michigan
Ann Arbor, MI 48109, USA

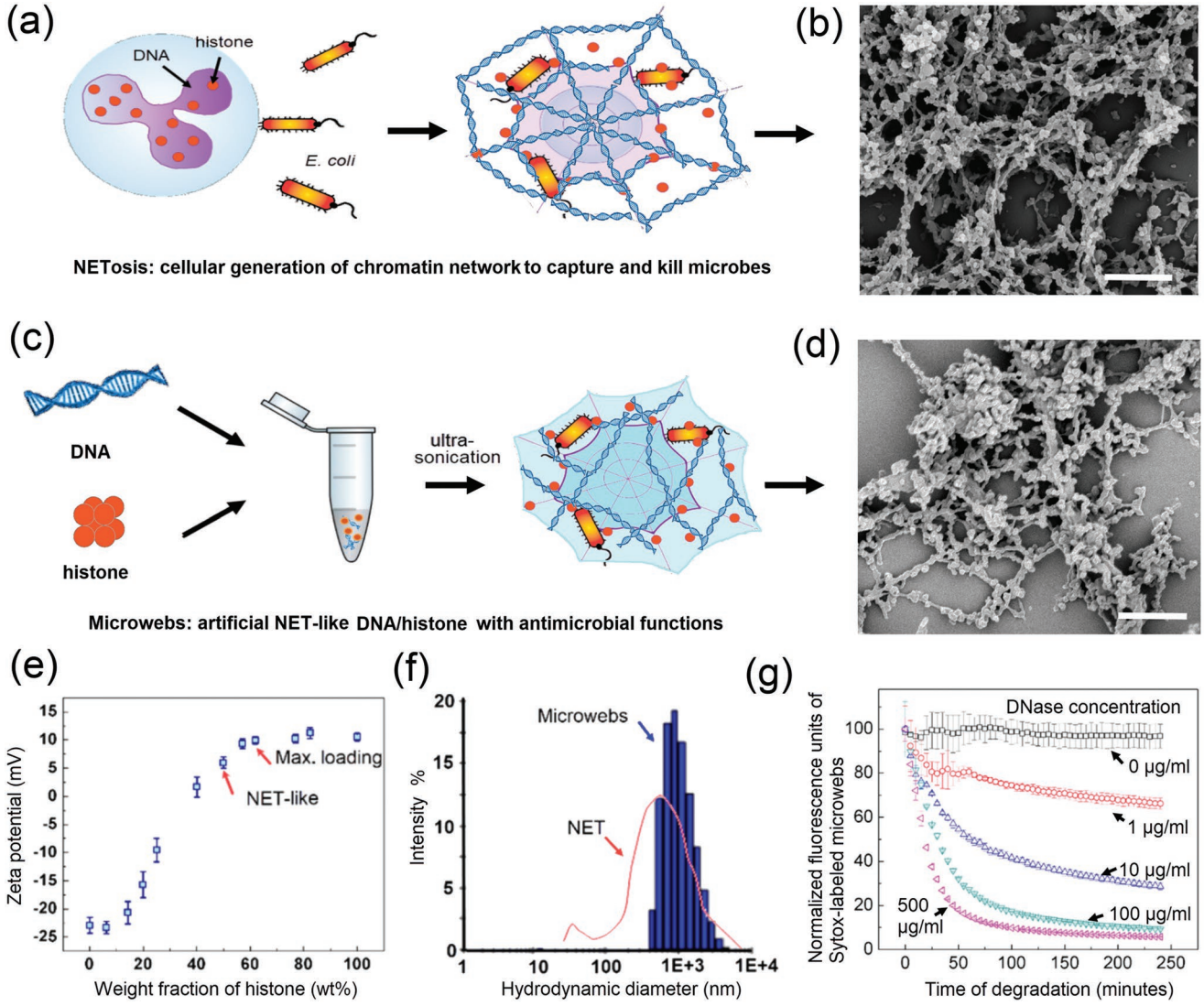

Figure 1. Synthesis and characterization of NET-like microwebs. a) Scheme and b) scanning electron microscopy illustrating NETs. c) Scheme and d) SEM illustrating microwebs. Scale bars = 1 μm. e) Zeta potentials and f) size distribution (DLS measurement) of microwebs. Size distribution of sonicated NETs is shown by the red curve. g) DNase-induced degradation of microwebs in HBSS. Microwebs were stained by SYTOX (Ex/Em = 488/523 nm).

because NETs were essential for the clearance of *E. coli*; moreover, the first clinical isolate of colistin-resistant bacteria harboring the mcr-1 gene in the US was *E. coli* from a urinary tract infection (UTI).[19] We evaluated the antimicrobial performance of NETs versus microwebs of different composition in comparative studies. We show how the microwebs trap *E. coli* and inhibit their growth as NETs do. In addition, we demonstrate that the microwebs can work synergistically with colistin sulfate to kill *E. coli*. Compared to isolation of NETs from neutrophils, our synthetic approach allows fast and larger-scale preparation of NET-like structures with well-defined compositions. This approach therefore provides a platform to study mechanisms of NET-bacteria interactions with less confounding factors to promote understanding of NET-related human diseases.

Inspired from decondensed chromatin structure of NETs, our synthetic "microwebs" were prepared by a sonicated mixture solution of DNA and histone (see the Experimental Section). Methylated lambda phage DNA was selected to formulate microwebs because its DNA length (48502 bp) is suitable for forming uniform and dispersible networks by sonication. At physiological DNA concentrations (≈100 μg mL^{-1}), shorter DNA only forms microparticles with histone in Hank's balanced salt solution (HBSS), while longer DNA results in large clumps that cannot be easily dispersed. After applying ultrasonication to the phage DNA/histone mixture, we obtained disassembled DNA-rich bundles decorated with histone-rich granules (Figure 1c,d). The resultant structure showed qualitative ultrastructural similarity to NETs collected from neutrophils. The thickness of the DNA bundles varied from 20 to 100 nm, in agreement with ultrafine nanostructures observed in NETs.[20] The formation of the microwebs is driven by the electrostatic complexation of DNA (zeta potential, $\zeta = -22$ mV) with

histone ($\zeta = +11.3$ mV). When the histone weight fraction in the microwebs, ω_{his}, was increased from 15 to 60 wt%, the DNA fibers were gradually covered by a coating of histone granules (Figure S1, Supporting Information), resulting in elevated zeta potentials (Figure 1e). When the histone fraction ω_{his} is above an upper limit of 60 wt%, the DNA-rich bundles were fully occupied by histone granules and therefore further attachment of histone to DNA was inhibited by electrostatic repulsion.

The maximum protein-loading capacity of the microwebs, $\omega_{his,max}$ = 60 wt%, is consistent with the reported fraction of all proteins in NETs (including histone, neutrophil elastase, cathepsin G, and other proteins) measured by mass spectrometry.[13] Microwebs with ω_{his} = 50 wt% acquire ultrafine structures like NETs. Dynamic light scattering (DLS) measurement of the sonicated microwebs suggests that the hydrodynamic diameter of the DNA bundles is comparable to that in NETs (Figure 1f). Due to the presence of histone, DNA colloids slowly aggregate and their hydrodynamic diameters increase over the time of aging (Figure S1, Supporting Information). Similar to NETs, the microwebs can be degraded by DNase *I* (Figure 1g).[6,21] The degradation rate of microwebs increased with the DNase concentration, as shown by the fluorescence quenching of the SYTOX-labeled microwebs after degradation of DNA (Figure 1g; Figure S2, Supporting Information).

Since the primary function of NETs is to trap bacteria,[6] we first tested the ability of microwebs to entrap the Gram-negative urinary pathogen, *E. coli UTI89*. Microwebs with different histone weight fractions, ω_{his} = 25%, 40%, 50%, and 57%, were employed as matrices to trap bacteria. To enable sufficient contact between *E. coli* and microwebs, we sequentially centrifuged the microwebs and bacteria so that the planktonic *E. coli* cells were forced onto the precipitated microwebs at time zero, $t = 0$ h. However, the temporarily attached *E. coli* can subsequently detach from the microwebs through bacterial movement. After 1 h of incubation, a near-steady-state bacterial entrapment was achieved, and the nonattached bacteria were removed by pipette washing. We observed that a higher density of *E. coli* cells was trapped on the positively charged microwebs than on the negatively charged and neutral microwebs, as shown by scanning electron microscopy (SEM) observation in **Figure 2**a–c. To quantify the number of entrapped bacteria, we prestained *E. coli* and then monitored the bacterial motion on microwebs for 1 h in HBSS. The entrapped *E. coli* cells were defined as those immobilized on microwebs without any observable motion, while the nonentrapped *E. coli* cells were

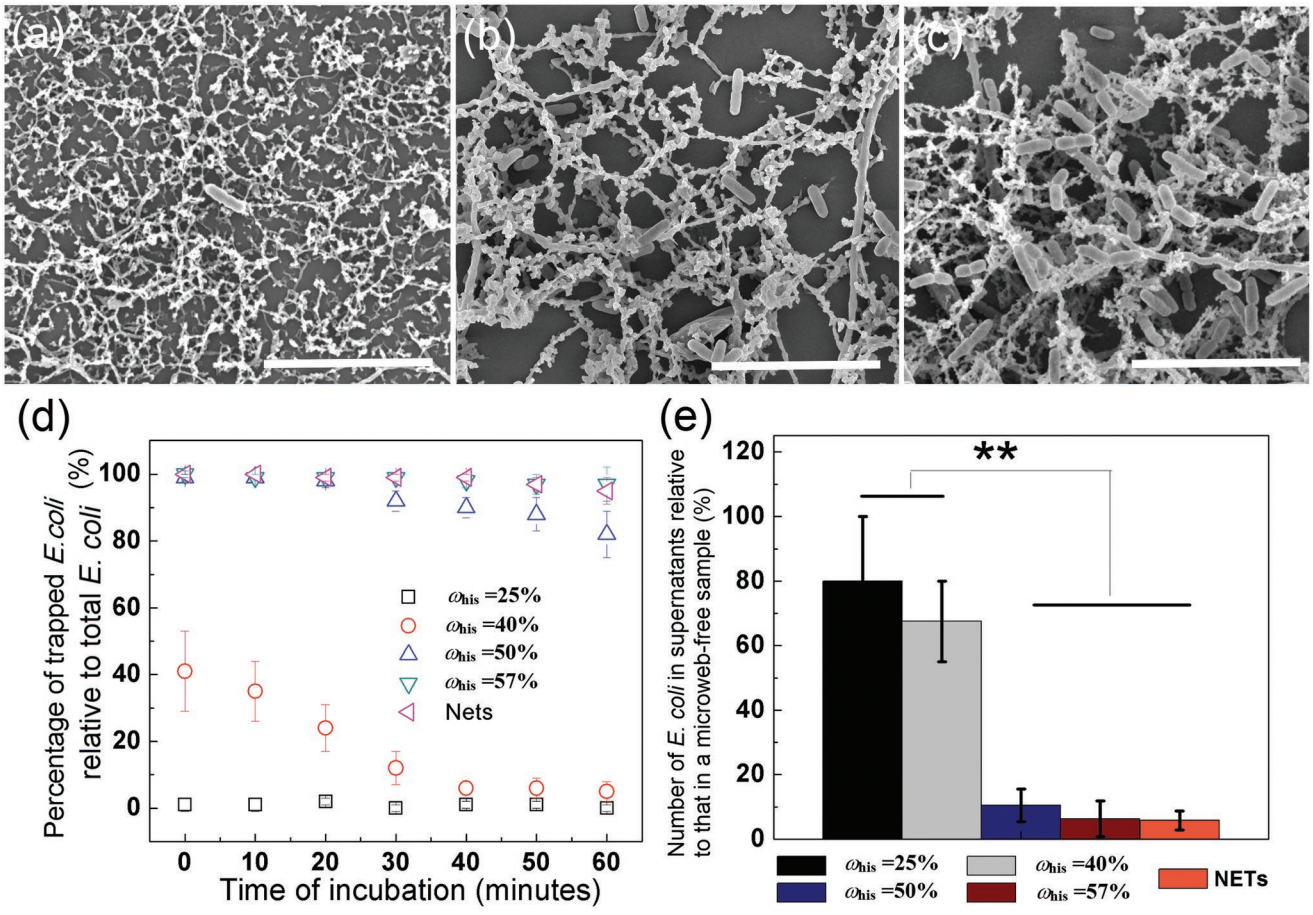

Figure 2. Entrapment of *E. coli* on microwebs. SEM images showing *E. coli* trapped on microwebs with a) $\zeta = -8$ mV, b) $\zeta = 0$ mV, and c) $\zeta = +6.5$ mV. Scale bars = 10 µm. d) The percentage of trapped *E. coli* on microwebs as a function of incubation time. e) The number of planktonic *E. coli* escaped from microwebs were counted by plating and colony forming unit enumeration. The percentage of planktonic *E. coli* is calculated from the ratio of *E. coli* in supernatants relative to that in NET-free control group. $^{**}P < 0.01$.

observed to self-rotate or swim to a different location under the microscope. After manually counting the number of motile and nonmotile *E. coli*, we found that 82% ± 4% (ζ = +5 mV, ω_{his} = 50%) and 93% ± 3% (ζ = +8 mV, ω_{his} = 57%) *E. coli* cells were trapped on microwebs with positive zeta potentials, in good agreement with the trapping observed on NETs (Figure 2d,e).[22] In contrast, less than 10% of *E. coli* cells were attached to the negatively charged (–9 mV) and near-neutral (–1 to +1 mV) microwebs. As the time of incubation increases, some *E. coli* cells initially attached to these microwebs were seen to detach. The membrane potential of these detached bacteria was elevated ($\zeta \approx 0$ mV) compared to the untreated *E. coli* (ζ = –12 mV). This is probably caused by either adaption of bacteria to microwebs or adsorption of histone to the bacterial cell wall. The detached *E. coli* cells in supernatant was further enumerated by serial dilution, plating, and colony counting. The results confirmed that positively charged microwebs efficiently inhibited the dispersion of *E. coli* as compared to negatively charged microwebs (Figure 2e). The charge-dependent bacterial trapping can be explained by an energy barrier set by the electrostatic interaction between the bacterial cell wall (e.g., lipopolysaccharide) and microwebs. A higher fraction of cationic histone (ω_{his} > 40%) in microwebs and therefore a higher electrostatic force enhanced the bacteria trapping efficiency.

To test if microwebs kill the trapped *E. coli*, we placed microwebs on top of *E. coli* cells through centrifugation and incubated the trapped *E. coli* for 1 h in HBSS. Subsequently, we removed the microwebs from *E. coli* cells by repeated washing and stained the remaining bacteria with the LIVE/DEAD BacLight bacterial viability kit. Using confocal laser scanning microscopy (CLSM), we found that most *E. coli* cells remained alive in microwebs and a small fraction were dead (red, **Figure 3**b). SEM observation reveals that live bacteria had intact capsules similar to those cultured in tryptic soy broth (TSB) (Figure 3f). Some of the microweb-entrapped *E. coli* cells were seen to shrink similar to those trapped on NETs (Figure 3g,h). The successful permeation of propidium iodide into these cells

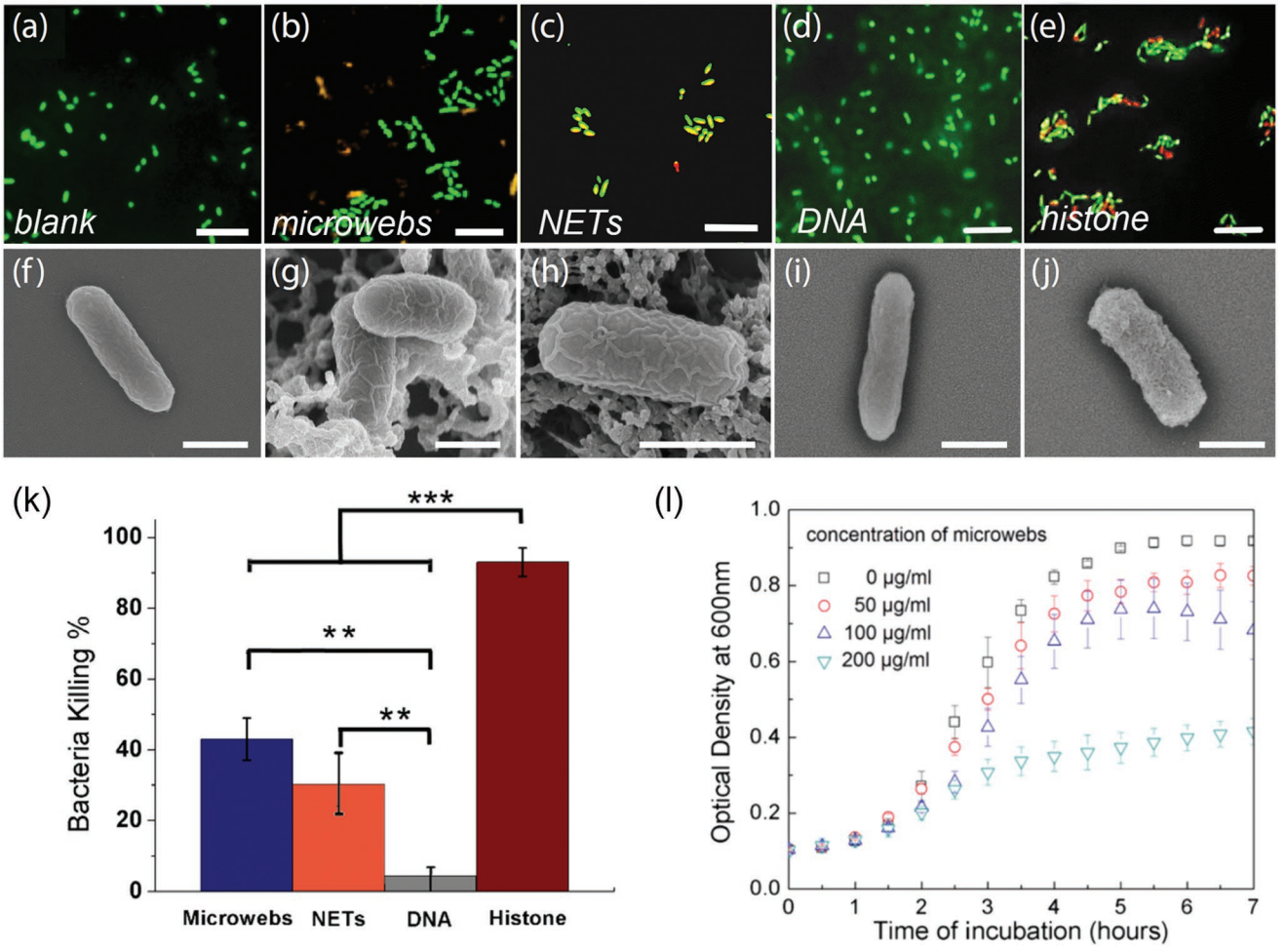

Figure 3. Viability assessment of *E. coli* cultured with microwebs. Fluorescence microscopy images of *E. coli* in a) tryptic soy broth, b) 100 μg mL^{-1} microwebs (ω_{his} = 50%), c) 100 μg mL^{-1} NETs, d) 50 μg mL^{-1} DNA solution, and e) 50 μg mL^{-1} histone solution (live cells: green; dead cells: red). Scale bars = 10 μm. The corresponding SEM images of *E. coli* cells cultured in indicated solutions are shown in (f) to (j). Scale bars = 1 μm. k) Microwebs reduce colony forming units of *E. coli* in HBSS. 10^5 *E. coli* cells were incubated in 100 μL microwebs (50 μg mL^{-1} DNA, ω_{his} = 50%), NETs (contains 50 μg mL^{-1} DNA, triggered by phorbol 12-myristate 13-acetate), 50 μg mL^{-1} DNA, and 50 μg mL^{-1} histone, respectively, for 1 h before transferred to agar plates. $^{**}P < 0.01$; $^{***}P < 0.001$. Growth curves of *E. coli* in a mixture of 100 μL microweb suspension and 100 μL TSB plus 1% glucose.

suggests loss of membrane integrity (Figure 3b). To determine which component in microwebs caused structural damage to *E. coli* cell wall, we separately cultured *E. coli* in the isolated DNA (Figure 3d,i) or histone solutions (Figure 3e,j). Within the range of physiologically relevant DNA concentrations (25–100 μg mL^{-1}), the viability of *E. coli* cells cultured in the DNA solution remained. In contrast, an increased cell death rate was observed after *E. coli* cells were cultured in a series of histone solutions with increasing protein concentration (25–100 μg mL^{-1}). SEM observation of these dead cells showed damaged capsules with nanosized pores. Previous studies have shown that histone H2B penetrates through *E. coli* membrane, and histone H3 and H4 can destruct bacterial cell wall.[23] To test if these membrane pores we observed are structural defects caused by dehydration of cells before SEM observation, we also used fluorescein isothiocyanate (FITC) to label histone and identify their bactericidal effect under CLSM. Our observation showed that FITC–histone alone can efficiently cause lysis of bacteria *E. coli* (Figure S3, Supporting Information). However, once complexed with DNA to form microwebs, the FITC–histones no longer break the cell membrane. Instead, these FITC–histones were absorbed on the *E. coli* cell wall.

To further quantify the antimicrobial potency of microwebs, we cultured *E. coli* in suspensions with microwebs (in HBSS) before they were diluted and transferred to agar plates for colony forming unit (CFU) enumeration (Figure 3k). The presence of microwebs (100 μg mL^{-1}) reduces CFU counts of *E. coli* (10^6 mL^{-1}) by 41% ± 8%, in agreement with the reduced CFU counts in the NETs group (32% ± 7%). By separately using DNA and histone as additives to culture medium, we confirmed that histone, rather than DNA, was the direct bactericidal component against *E. coli*. When *E. coli* were cultured in a nutrient-rich medium of 50 vol% TSB and 50 vol% HBSS containing microwebs (Figure 3l), we did not observe an immediate decline in the bacterial proliferation rate within the first 2 h, perhaps due to the diffusion-limited penetration of histone through the *E. coli* cell wall. However, microwebs reduced the overall *E. coli* cell number in the stationary phase (t = 4–6 h), which is attributed to the trapping and mild killing effects of the microwebs. After microwebs were dismantled by DNase *I*, the remaining structures no longer inhibit bacterial growth in the stationary phase (Figure S4, Supporting Information). Our observation suggests that the network of DNA nanofibers also contributes to the antimicrobial potency of the microwebs, in agreement with previous reports on DNase-induced loss of antimicrobial potency of NETs.[6,10,11] The supernatant resulting from preparation of microwebs does not significantly change the growth curve of *E. coli* (Figure S4, Supporting Information), suggesting that free histone remaining in the supernatant is trivial. The antimicrobial mechanism of action of the microwebs, therefore, mainly relies on their direct contact with bacteria. Some of the entrapped *E. coli* cells exhibited phenotype changes, such as filamentous growth (Figure S5, Supporting Information). Filamentation is generally considered a protective strategy for bacteria to evade stressed conditions, such as antibiotic treatment and phagocytosis of macrophages.[24] In view of the responses of *E. coli* to microwebs, we propose that microwebs are bacteriostatic networks with functions of trapping and moderate inhibition of *E. coli* proliferation.

As a structural and chemical analogue of NETs, microwebs can be used for convenient screening of antibiotics which may function cooperatively with physiologically-produced NETs. To test this hypothesis, we measured the tolerance of *E. coli* to different antibiotics with and without microwebs (ω_{his} = 50%). Four clinically potent antibiotics for urinary tract infection, including amoxicillin, colistin sulfate, nitrofurantoin, and trimethoprim were tested. In HBSS, the antimicrobial potency of amoxicillin and colistin sulfate was significantly enhanced in the presence of microwebs (100 μg mL^{-1}), as shown by quantitative culture in **Figure 4**a,b. This antibacterial enhancement was also identified by determining the minimum inhibitory concentration (MIC) by standard broth microdilution for each antibiotic with and without microwebs. Without addition of microwebs, the MICs of colistin sulfate and amoxicillin are 3 and 12 μg mL^{-1}, respectively. With addition of microwebs, the MICs for colistin sulfate and amoxicillin were reduced to 0.75 and 6 μg mL^{-1}, respectively. Similar antimicrobial enhancement was also observed when enumerating the CFU counts of colistin-resistant *E. coli* strain IHD86_4 (+*mcr-1*) in HBSS (Figure S6, Supporting Information). Colistin is a last resort antibiotic used against multidrug resistant *E. coli* that has a side effect of frequently causing acute kidney injury.[25] Dosing at a level that is bactericidal while minimizing risk of kidney injury is an important clinical challenge. Our results suggest an interesting possibility that endogenous NETs may assist colistin in fighting bacteria in vivo, allowing for the use of lower doses than may seem necessary with conventional in vitro antibiotic susceptibility tests performed in the absence of NETs. Interestingly, colistin has been reported to sensitize human neutrophil-induced killing of resistant *E. coli* in vivo.[26]

From the growth curve of *E. coli* with colistin treatment, we observed that the slope of the exponential phase, which was not affected by colistin treatment alone (Figure 4c), decreased with increasing concentrations of colistin in the presence of microwebs (Figure 4d). As colistin sulfate disrupts the bacterial membrane,[27] the decreased slope of the exponential growth phase may be explained by the enhanced permeability of the bacterial cell wall induced by histone. In comparison, the slopes of the exponential phase for the amoxicillin-treated *E. coli* were less affected by amoxicillin concentration, regardless of the presence of microwebs (Figure 4e,f). Amoxicillin can inhibit the synthesis of cell wall but does not disrupt the cell membrane; therefore, with the unchanged membrane permeability to histone, the slope of exponential phase does not change even with increased concentration of amoxicillin (Figure 4f) when it is below the MIC. Additionally, microwebs did not change the MIC for nitrofurantoin and trimethoprim (see Figure S7 in the Supporting Information), as nitrofurantoin targeted ribosomal proteins and trimethoprim inhibited DNA synthesis.[28] Our results suggest that microwebs can collaboratively work with antibiotics that targets the bacterial cell envelope.

In summary, we synthesized NET-like microwebs through sonochemical complexation of DNA and histone. To the best of our knowledge, this is the first report demonstrating that manipulation on the morphology and composition of DNA–histone complex can achieve antimicrobial functions similar to endogenous NETs. By varying the ratio of DNA to histone, we correlated the bacteria trapping and antimicrobial properties

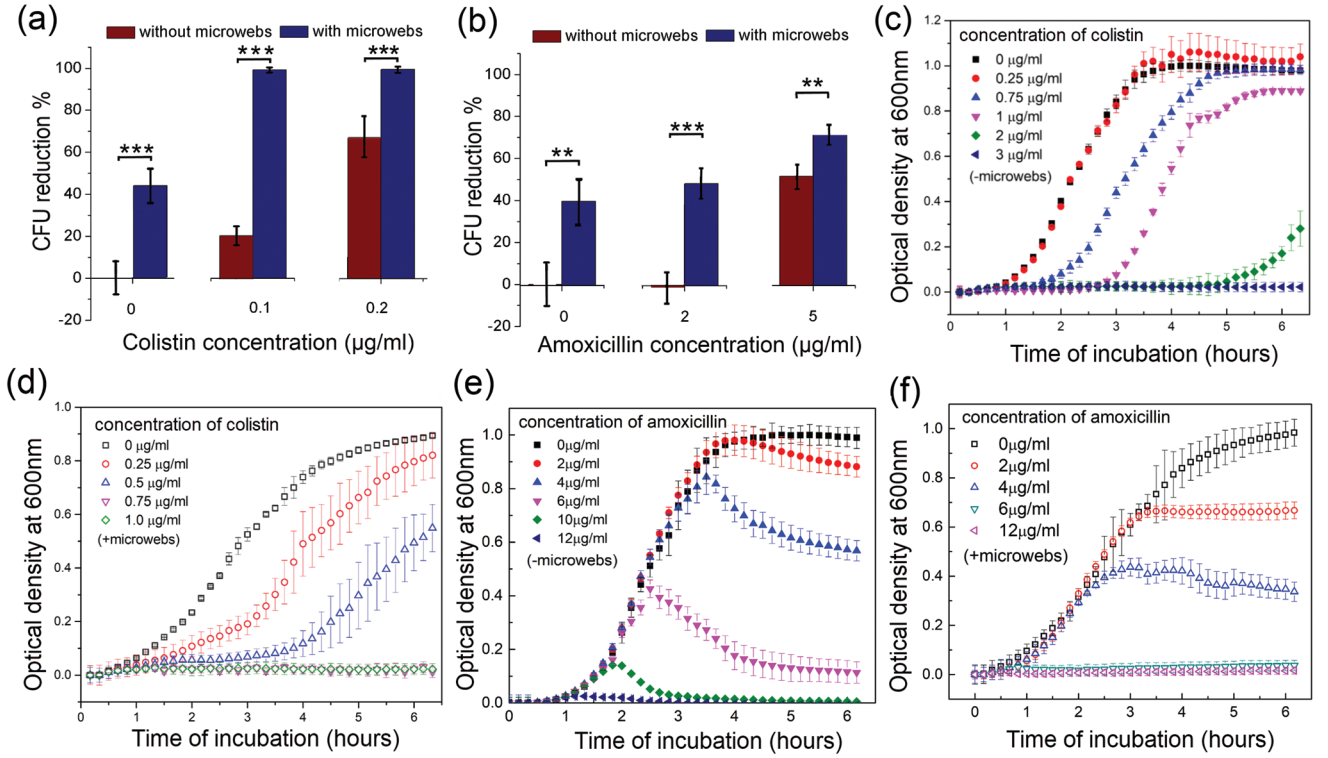

Figure 4. Microwebs can work cooperatively with antibiotics against *E. coli*. CFU counting of *E. coli* (inoculum = 10^5 cells) after culture in a 100 μL HBSS containing 100 μg mL^{-1} microwebs (ω_{his} = 50%) plus antibiotics: a) colistin and b) amoxicillin for 1 h at 37 °C. Comparisons on the growth curves of *E. coli* (inoculum = 10^6 cells) cultured in a mixture solution of 100 μL TSB, 100 μL HBSS, microwebs, and antibiotics: c) with colistin, without microwebs; d) with colistin, with 50 μg mL^{-1} microwebs; e) with amoxicillin, without microwebs; and f) with amoxicillin, with 50 μg mL^{-1} microwebs. $^{**}P < 0.01$; $^{***}P < 0.001$.

of the microwebs with regards to their DNA to histone ratio. This synthetic approach provides a flexible platform to quantitatively study the physiology role of different NET components. The compositionally minimalistic microwebs efficiently trap *E. coli* through electrostatic forces to an extent similar to NETs. DNase-mediated degradation experiments demonstrate that the network of DNA nanofibers also contribute to the inhibition of bacterial proliferation. *E. coli* exhibited filamentous growth, a well-known adaptive response, when exposed to both microwebs and NETs. Interestingly, microwebs work collaboratively with the last-resort antibiotic colistin and target bacterial cell-envelope, including colistin-resistant *E. coli* (IHD86_4 *mcr-1*). These results show that microwebs are useful for studying bacteria-NET interactions and for screening of antimicrobials that works collaboratively with physiologically-produced NETs.[29] Since DNA-based NETs are also associated with pathology of some autoimmune diseases,[12] further studies on microwebs should address their correlations with human disease or guide further efforts to design non-DNA based artificial NETs for clinical tests.

Experimental Section

Preparation of Microwebs: Microwebs was prepared by spontaneous polymerization of methylated lambda phage DNA in the presence of histone. Calf thymus histone (Sigma, H9250) and methylated lambda phage DNA (Sigma, D3779) were separately dissolved and diluted in HBSS. The DNA (100–400 μg mL^{-1}) and histone concentration were measured from Nanodrop 2000c. To prepare microwebs, the DNA solution (100 μL, 100–400 μg mL^{-1}) was mixed with histone (100 μL) solutions using an ultrasonic homogenizer (Qsonica Q125 sonicator, intensity set 20%) for 15 s. Depending on the weight fraction of histone in microwebs, the concentration of histone was varied from 33 to 400 μg mL^{-1}. As a comparison, NETs isolated from neutrophils (see the experimental details in the Supporting Information) were dispersed into HBSS by sonication under the same conditions (intensity set 20%, last for 15 s).

Characterization: The zeta potentials of microwebs (DNA: 50 μg mL^{-1}) were measured using a zetasizer (Malvern) at 37 °C. Their size distribution was measured using Wyatt DynaPro NanoStar Dynamic Light Scattering. NETs formed from neutrophils were dispersed into HBSS by sonication for 15 s before DLS measurement. Morphology of microwebs (with and without *E. coli*) were imaged using scanning electron microscopy (Hitachi SU8230, U_{acc} = 1 kV, I = 15 mA). The SEM samples were fixed by 4% paraformaldehyde, washed with deionized water, and sequentially dehydrated in 25, 50, 75, 95, and 100 vol% ethanol. Subsequently, samples were immersed in hexamethyldisilane and vacuumed overnight. Dried samples were sputter-coated with gold nanoparticles (SPI-Module 60s, 18 mA).

Degradation: Suspension of microwebs (100 μL, preheated to 37 °C) was prestained with SYTOX green (1×10^{-6} M) and mixed with DNase solutions (bovine pancreas DNase I, Sigma 11284932001, diluted in HBSS) at equal volumes. The final concentration of DNase was 1, 10, 100, and 500 μg mL^{-1}. Degradation of the microwebs was monitored in a Synergy Neo2 Multi-mode microplate reader (BioTek, Ex/Em = 488/523 nm) at 37 °C for 4 h.

Bacterial Media and Growth Conditions: E. coli UTI89 was streaked on a tryptic soy agar (TSA, Sigma 22091) plate and incubated at 37 °C

overnight. One colony was scratched from TSA plate and suspended in 1 mL tryptic soy broth (Sigma 22092) with 1% glucose, until the optical density at 600 nm (OD_{600}) of the cultures reached 0.3–0.6. The *E. coli* suspension was diluted to $OD_{600} = 0.01$.

Bacteria-Trapping Assay: Suspension of microwebs (100 µL, containing 50 µg mL^{-1} DNA) was pipetted into 96-well microplates and centrifuged (4000 rpm, 10 min). *E. coli* culture (100 µL, $OD_{600} = 0.01$ in HBSS) prestained with SYTO 9 was added on top of the microwebs and centrifugated (4000 rpm, 10 min). Motion of *E. coli* was continuously monitored for 1 h using fluorescence microscopy (Nikon Eclipse 80i). The percentage of trapped *E. coli* is expressed as the ratio of nonmotile *E. coli* to the total number of bacteria. After 1 h of incubation at 37 °C, the planktonic *E. coli* in the supernatant was collected, serial diluted by tenfold using HBSS, and transferred to agar plates. After overnight incubation, the *E. coli* colonies were numerated.

Cell Viability Assay: Suspension of *E. coli* cells (100 µL, $OD_{600} = 0.01$ in HBSS) was allocated into a 96-well microplate and centrifugated (4000 rpm, 10 min). Afterward, suspension of microwebs (100 µL) was slowly injected on top of cells and centrifuged (4000 rpm, 10 min). After 1 h of incubation (37 °C), the microwebs on top of *E. coli* were removed by repeated pipette washing (HBSS) for 3–5 times. The *E. coli* cells attached to the microplate substrate were stained (0.5 vol% 3.34×10^{-3} M SYTO 9 and 0.5 vol% 20×10^{-3} M propidium iodide, 15 min, Thermofisher L7012), washed with deionized water, and imaged via fluorescence microscopy (Nikon Eclipse 80i, Nikon A1Rsi).

Bacteria Proliferation Assay: Proliferation of *E. coli* was measured from OD_{600} of the bacteria culture suspension using a plate reader (Biotek). 100 µL TSB containing 10^6 *E. coli* cells were mixed with 100 µL microwebs (in HBSS, w_{his} = 50%) at different concentrations of 0, 25, 50, and 100 µg mL^{-1}. *E. coli* were cultured at 37 °C for 7 h and their corresponding OD_{600} values were measured (OD_{600} of microweb suspension without *E. coli* was subtracted as background). Three independent bacteria colonies were used. Data are presented as mean values ± S.D.

Quantitative Culture: 10^5 *E. coli* cells (in 10 µL HBSS) were mixed with suspension of microwebs (100 µL, 100 µg mL^{-1} in HBSS) and incubated for 1 h (37 °C). Next, 10 µL mixture was extracted from each sample and diluted with HBSS at a volumetric ratio of 1:1000. Subsequently, 10 µL of the diluted solution samples was spotted onto the agar plate; this liquid transfer was repeated 6 times for each sample. The spotted agar plate was incubated at 37 °C for 12 h. The numbers of CFUs were then enumerated. Four different *E. coli* colonies were tested for CFU enumeration, and unpaired Student's *t*-test was employed to quantify the statistical significance using *P*-values.

Antibiotic Tests: Four antibiotics were separately dissolved in deionized water as stock solutions (colistin, Sigma, PHR1605 20 µg mL^{-1}; amoxicillin, Sigma, PHR1127, 400 µg mL^{-1}; trimethoprim, Sigma, PHR1056 200 µg mL^{-1}; nitrofurantoin, Sigma, PHR1191, 1 mg mL^{-1}). These antibiotics were diluted in either suspension of microwebs or HBSS to desired concentrations. For quantitative culture, 10^5 cells were suspended in a mixture of 100 µL HBSS (with and without 100 µg mL^{-1} microwebs) and 100 µL antibiotic solution. For growth curves, 10^6 cells were seeded in a mixture of 100 µL TSB, 100 µl HBSS (with and without 100 µg mL^{-1} microwebs microwebs) and antibiotics. Quantitative culture and growth curves were performed following the same protocols as above. The MIC was determined by standard broth microdilution. 10^6 cells mL^{-1} were inoculated into increasing concentrations of antibiotic ± microwebs. After 16-h incubation at 37 °C, the MIC was identified as the lowest concentration with no visible bacterial growth.

Supporting Information

Supporting Information is available from the Wiley Online Library or from the author.

Acknowledgements

This research project was funded by the National Institutes of Health (NIH NIAID U19 AI116482, R01 AI141883, and K08 AI128006; NIGMS R01 GM123517; NHLBI R01 HL134846; and U01 CA210152), the Veterans Administration (Merit award BX-002788), and a Burroughs Wellcome Fund Investigator in the Pathogenesis of Infectious Disease award.

Conflict of Interest

The authors declare no conflict of interest.

Keywords

antibiotic resistance, bacteria *E. coli,* biomimetic materials, DNA nanofiber networks, neutrophil extracellular traps

Received: November 17, 2018
Revised: January 16, 2019
Published online: January 30, 2019

[1] T. A. Blackledge, N. Scharff, J. A. Coddington, T. Szüts, J. W. Wenzel, C. Y. Hayashi, I. Agnarsson, *Proc. Natl. Acad. Sci. USA* **2009**, *106*, 5229.
[2] a) D. K. V. Kumar, S. H. Choi, K. J. Washicosky, W. A. Eimer, S. Tucker, J. Ghofrani, A. Lefkowitz, G. McColl, L. E. Goldstein, R. E. Tanzi, R. D. Moir, *Sci. Transl. Med.* **2016**, *8*, 340ra72; b) U. Shimanovich, I. Efimov, T. O. Mason, P. Flagmeier, A. K. Buell, A. Gedanken, S. Linse, K. S. Åkerfeldt, C. M. Dobson, D. A. Weitz, T. P. Knowles, *ACS Nano* **2015**, *9*, 43.
[3] L. Drago, M. Bortolin, C. Vassena, S. Taschieri, M. Del Fabbro, *BMC Microbiol.* **2013**, *13*, 47.
[4] V. Brinkmann, A. Zychlinsky, *Nat. Rev. Microbiol.* **2007**, *5*, 577.
[5] V. Papayannopoulos, K. D. Metzler, A. Hakkim, A. Zychlinsky, *J. Cell Biol.* **2010**, *191*, 677.
[6] a) V. Brinkmann, U. Reichard, C. Goosmann, B. Fauler, Y. Uhlemann, D. S. Weiss, Y. Weinrauch, A. Zychlinsky, *Science* **2004**, *303*, 1532; b) R. L. Young, K. C. Malcolm, J. E. Kret, S. M. Caceres, K. R. Poch, D. P. Nichols, J. L. Taylor-Cousar, M. T. Saavedra, S. H. Randell, M. L. Vasil, J. L. Burns, *PLoS One* **2011**, *6*, e23637.
[7] C. F. Urban, U. Reichard, V. Brinkmann, A. Zychlinsky, *Cell. Microbiol.* **2006**, *8*, 668.
[8] C. N. Jenne, C. H. Wong, F. J. Zemp, B. McDonald, M. M. Rahman, P. A. Forsyth, G. McFadden, P. Kubes, *Cell Host Microbe* **2013**, *13*, 169.
[9] A. B. Guimarães-Costa, M. T. Nascimento, G. S. Froment, R. P. Soares, F. N. Morgado, F. Conceição-Silva, E. M. Saraiva, *Proc. Natl. Acad. Sci. USA* **2009**,*106*, 6748.
[10] a) F. Wartha, K. Beiter, B. Albiger, J. Fernebro, A. Zychlinsky, S. Normark, B. Henriques-Normark, *Cell. Microbiol.* **2007**, *9*, 1162; b) F. Ma, L. Yi, N. Yu, G. Wang, Z. Ma, H. Lin, H. Fan, *Front. Cell. Infect. Microbiol.* **2017**, *7*, 86.
[11] a) R. Menegazzi, E. Decleva, P. Dri, *Blood* **2012**, *119*, 1214; b) V. Thammavongsa, D. M. Missiakas, O. Schneewind, *Science* **2013**, *342*, 863.
[12] a) V. Marcos, Z. Zhou, A. Ö. Yildirim, A. Bohla, A. Hector, L. Vitkov, E. M. Wiedenbauer, W. D. Krautgartner, W. Stoiber, B. H. Belohradsky, N. Rieber, *Nat. Med.* **2010**, *16*, 1018; b) V. Papayannopoulos, *Nat. Rev. Immunol.* **2018**, *18*, 134.
[13] C. F. Urban, D. Ermert, M. Schmid, U. Abu-Abed, C. Goosmann, W. Nacken, V. Brinkmann, P. R. Jungblut, A. Zychlinsky, *PLoS Pathog.* **2009**, *5*, e1000639.
[14] C. Mottola, D. Romeo, *J. Cell Biol.* **1982**, *93*, 129.

[15] S. R. Clark, A. C. Ma, S. A. Tavener, B. McDonald, Z. Goodarzi, M. M. Kelly, K. D. Patel, S. Chakrabarti, E. McAvoy, G. D. Sinclair, E. M. Keys, *Nat. Med.* **2007**, *13*, 463.
[16] B. G. Yipp, B. Petri, D. Salina, C. N. Jenne, B. N. Scott, L. D. Zbytnuik, K. Pittman, M. Asaduzzaman, K. Wu, H. C. Meijndert, S. E. Malawista, *Nat. Med.* **2012**, *18*, 1386.
[17] J. P. Frampton, M. Tsuei, J. B. White, A. T. Abraham, S. Takayama. *Biotechnol. J.* **2015**, *10*, 121.
[18] a) Y. Liu, M. Guthold, M. J. Snyder, H. Lu, *Colloids Surf., B* **2015**, *134*, 17. b) L. A. Lanier, H. Bermudez, *Macromol. Rapid Commun.39*, 1800342; c) M. Roushan, M. Jorfi, A. Mishra, K. H. K. Wong, J. Jorgensen, E. Ell, J. F. Markmann, J. Lee, D. Irimia. *Adv. Biosyst.2*, 1800040.
[19] a) T. H. Ng, M.-H. Wu, S.-H. Chang, T. Aoki, H.-C. Wang, *Dev. Comp. Immunol.* **2015**, *48*, 229; b) R. J. Meinersmann, S. R. Ladely, J. R. Plumblee, M. C. Hall, S. A. Simpson, L. L. Ballard, B. E. Scheffler, L. L. Genzlinger, K. L. Cook, *Genome Announce.* **2016**, *4*, e00898.
[20] a) R. H. Pires, S. B. Felix, M. Delcea, *Nanoscale* **2016**. *8*, 14193; b) R. Manzenreiter, F. Kienberger, V. Marcos, K. Schilcher, W. D. Krautgartner, A. Obermayer, M. Huml, W. Stoiber, A. Hector, M. Griese, M. Hannig, *J. Cystic Fibrosis* **2012**, *11*, 84.
[21] V. Papayannopoulos, D. Staab, A. Zychlinsky, *PLoS One* **2011**, *6*, e28526.
[22] a) M. Floyd, M. Winn, C. Cullen, P. Sil, B. Chassaing, D. Yoo, A. T. Gewirtz, J. B. Goldberg, L. L. McCarter, B. Rada. *PLoS Pathog.* **2016**, *12*, e1005987. b) V. Brinkmann, A. Zychlinsky, *J. Cell Biol.* **2012**, *198*, 773.
[23] a) J. G. Hirsch, *J. Exp. Med.* **1958**, *108*, 925. b) C. Tagai, S. Morita, T. Shiraishi, K. Miyaji, S. Iwamuro, *Peptides* **2011**, *32*, 2003.
[24] a) Y. Yu, K. Kwon, T. Tsitrin, S. Bekele, P. Sikorski, K. E. Nelson, R. Pieper, *PLoS Pathog.* **2017**, *13*, e1006151; b) S. S. Justice, D. A. Hunstad, P. C. Seed, S. J. Hultgren, *Proc. Natl. Acad. Sci. USA* **2006**, *103*, 19884.
[25] L. Dalfino, F. Puntillo, M. J. M. Ondok, A. Mosca, R. Monno, S. Coppolecchia, M. L. Spada, F. Bruno, N. Brienza. *Clin. Infect. Dis.* **2015**, *61*, 1771.
[26] F. Rose, K. U. Heuer, U. Sibelius, S. Hombach-Klonisch, L. Kiss, W. Seeger, F. Grimminger. *J. Infect. Dis.* **2000**, *182*, 191.
[27] J. Li, R. L. Nation, R. W. Milne, J. D. Turnidge, K. Coulthard, *Int. J. Antimicrob. Agents* **2005**, *25*, 11.
[28] M. Koike, K. Iida, MatsuoT. *J. Bacteriol.* **1969**, *97*, 448.
[29] M. W. Munks, A. S. McKee, M. K. MacLeod, R. L. Powell, J. L. Degen, N. A. Reisdorph, J. W. Kappler, P. Marrack, *Blood* **2010**, *116*, 5191.